Aerosol Science and Technology

ISSN: 0278-6826 (Print) 1521-7388 (Online) Journal homepage: https://www.tandfonline.com/loi/uast20

Categorization of Lung Morphology Based on FRC and Height: Computer Simulations of Aerosol Deposition

M. Pichelin , G. Caillibotte , I. Katz & T. Martonen

To cite this article: M. Pichelin , G. Caillibotte , I. Katz & T. Martonen (2012) Categorization of Lung Morphology Based on FRC and Height: Computer Simulations of Aerosol Deposition, Aerosol Science and Technology, 46:1, 70-81, DOI: 10.1080/02786826.2011.605816

To link to this article: https://doi.org/10.1080/02786826.2011.605816

Aerosol Science and Technology, 46:70–81, 2012

ISSN: 0278-6826 print / 1521-7388 online
DOI: 10.1080/02786826.2011.605816

Categorization of Lung Morphology Based on FRC and Height: Computer Simulations of Aerosol Deposition

M. Pichelin,[1] G. Caillibotte,[1] I. Katz,[1,2] and T. Martonen[3]

[1]*Medical Gases Group, Air Liquide Santé International, Centre de Recherche Claude-Delorme, Jouy-en-Josas, Paris, France*
[2]*Department of Mechanical Engineering, Lafayette College, Easton, Pennsylvania, USA*
[3]*CyberMedicine, Laguna Beach, California, USA*

The aim of this study was to compare the human subject experimental measurements of particle deposition within the lungs using the aerosol bolus technique with the results of analytical modeling as a basis for assessing the influence of lung morphology on inhaled particle deposition patterns. A methodology for scaling the lung morphology, based on a classic symmetric dichotomous model, as a function of both functional residual capacity and height of the investigated population is presented. Because of the availability of deposition data for male and female lung morphologies, these were used as an example to address the importance of adjusting lung morphology in calculating the aerosol deposition rates. In order to represent the 2 groups based on gender enrolled in the experimental study, 2 lung morphologies have been built. An analytical and mechanistic model was used to mimic the bolus delivery technique and simulate the aerosol deposition in each of the 2 groups. Predicted results were compared with experimental data for both total deposition fraction and bolus recovery (fraction of exhaled particles compared with inhaled particles) for 3 flow rates and 3 particle sizes. Good agreement was found between theoretical and measured data, showing the primary importance of the differentiation of the lung morphology to predict the aerosol deposition within human lungs. This study presents a morphological lung model that is adaptable to specific populations (e.g., gender or race), groups (e.g., a clinical study population), or even individuals.

INTRODUCTION

Inhalation therapies based on aerosolized drugs are widely employed in the treatment of respiratory diseases. By targeting appropriate deposition sites within human lungs, the efficacies of inhaled pharmacologic agents could be improved and their associated side effects reduced (Labiris and Dolovich 2003). This optimization of deposition can be realized by controlling aerosol properties (e.g., diameters or material densities) and/or regulating breathing patterns (Heyder 2004). Hence, by producing an aerosol with a desired particle size distribution, the effectiveness of a treatment can be either maintained while minimizing harmful systemic exposure (Howarth 2001) or improved via a modification of the clinical response due to an optimization of regional particle deposition within lungs (Pritchard 2001), i.e., targeting.

When using lungs as the portal of entry into the body, it is important that the physical factors affecting the behavior and fate of inhaled particles be understood to optimize the aerosol deposition within the respiratory tract (Martonen 1993; Finlay and Martin 2008). As such, aerosol deposition has been thoroughly investigated using 3-dimensional (3D) computational fluid dynamics (CFD) simulations of flow patterns and particle transport and deposition (Katz and Martonen 1996; Martonen et al. 2005b; Vial et al. 2005; Longest and Vinchurkar 2007; Farkas and Balashazy 2008; Xi et al. 2008). Analytical modeling is an alternative to these 3D CFD methods. Various predictive models have been developed. They are based on the description of the deposition efficiency of particles by 3 main mechanisms: diffusion, sedimentation, and inertial impaction. Other models are based on empirical correlations (Martin and Finlay 2006; Finlay and Martin 2008) or use a semiempirical approach to describe the values of regional deposition (ICRP 1994). A third group of models uses the stochastic equations to predict the deposition of polydisperse aerosol within a symmetric structure of the human lung (Martonen 1993) or monodisperse aerosol in an asymmetric lung structure (Anjilvel and Asgharian 1995; Asgharian et al. 2001). Dynamic transport models including a set of time-variant transport equations to estimate the particle deposition in a symmetric lung model have also been developed (Taulbee and Yu 1975; Darquenne and Paiva 1994; Choi and Kim 2007).

Received 4 February 2011; accepted 29 June 2011.
The authors gratefully acknowledge Dr. Alexandre Makarenko for his significant contribution to this work.
Address correspondance to M. Pichelin, Medical Gases Group, Air Liquide Santé International, Centre de Recherche Claude-Delorme, 1, chemin de la porte des Loges, Les Loges-en-Josas, BP126, 78354 Jouy-en-Josas Cedex, France. E-mail: marine.pichelin@airliquide.com

For targeting the purpose, the prediction of aerosol deposition may need to take into account some patients' individual characteristics, which implies the simulation of nonacademic breathing patterns and individualization of lung morphology including pathology (Phalen et al. 1990; Oldham 2010). Indeed, large intersubject variabilities in particle deposition have been shown by various experiments (Stahlhofen et al. 1981; Heyder et al. 1982) even in healthy subjects.

The lung structure for an individual is very rarely known. Nevertheless, reference data, such as the functional residual capacity (FRC), can be used to adapt the morphological models for individuals or populations (in terms of age, gender, and ethnicity). On the basis of the FRC and height, we have developed a methodology using nonmonotonous scaling of the airways' length and diameter and alveolar volume, to build adapted lung morphologies. This study represents a first step toward model individualization through the process of lung morphology categorization: the distinction between male and female lungs, based on the physiological parameters. In order to estimate the relevance and applicability of our method to aerosol therapy, we compared our simulated results with experimental data from the literature.

The lung deposition of aerosols can be measured by a variety of methods (Kim 2000) with various levels of detail and accuracy. Hence, many experimental studies have been conducted to measure the total deposition fraction (TDF, i.e., fraction of deposited to inhaled particles) in healthy adult subjects for a large scope of particle sizes and breathing patterns (Heyder et al. 1975; Heyder et al. 1982; Heyder et al. 1986; Muir and Cena 1987; Schiller et al. 1988; Bennett et al. 1996; Bennett et al. 1997; Jaques and Kim 2000; Brown et al. 2002; Kim and Jaques 2004, 2005; Kim and Hu 2006). Regional deposition, which is of particular interest when considering targeting drug delivery, has been investigated by several laboratory teams (Stahlhofen et al. 1980; Stahlhofen et al. 1981; Heyder et al. 1986; Pritchard et al. 1986; Bennett et al. 1998; Bennett et al. 1999). The method for splitting the intrathoracic deposition into tracheobronchial (TB) tree and pulmonary (PU) deposition is based on the noninvasive external detection of tracer material during several hours after inhalation. The clearance mechanism is considered to be much slower in the nonciliated air spaces (alveolar zone) than in the ciliated airways (TB region). However, a large intersubject variability in TB clearance rates exists (Stuart 1984) and the mucociliary clearance may not truly represent the TB deposition (Kim et al. 1996). Other techniques can be used to assess the regional deposition. The aerosol bolus delivery technique, initially designed as a diagnostic tool, provides very useful information on the repartition of deposited particles within the lungs (Kim et al. 1996; Bennett et al. 1998; Kim and Hu 1998; Bennett et al. 1999; Peterson et al. 2008). Among these experimental studies, only the work conducted by Kim and Hu (1998) investigated the differences in regional aerosol deposition in male and female populations. Other authors have examined the influence of gender on aerosol deposition in human lungs; however, the experimental conditions of some of these analyses were impossible to simulate because of missing information. Other studies analyze only the TDF of aerosol (Jaques and Kim 2000; Kim and Hu 2006); as our goal is to develop a mathematical model to optimize drug delivery, these TDF values are insufficient to address the targeting.

Consequently, the dataset collected by Kim and Hu (1998) (henceforth referred to as the KH experiments) represents a unique source of published information on deposition assessed by aerosol bolus delivery in both male and female groups. This is of great interest for our study that aims at comparing experimental values with predicted results obtained with our simulation program for 2 different populations (i.e., male and female). This study should provide further guidance regarding the distinction of human subject subpopulations, in general, in the treatment of respiratory diseases and inhaled therapies.

METHODS

Description of the Theoretical Model

The analytical code used in our study predicts aerosol deposition distribution within the respiratory tract and is based on the methodology proposed by Martonen (1982). This well-known code has been favorably compared with experimental results from human subject exposures (Martonen and Katz 1993; Martonen et al. 2000; Martonen et al. 2005a) and applied with different healthy and diseased lung morphologies (Martonen 1993; Martonen et al. 1995; Katz et al. 2001; Segal et al. 2002; Sbirlea-Apiou et al. 2004). It considers the human lung as a dichotomous hierarchy of symmetrical tubes wherein the particle deposition is caused by 3 physical phenomena: inertial impaction, sedimentation, and diffusion. Analytical expressions are used to assess the particle deposition efficiencies inside lung airways due to those 3 mechanisms (Ingham 1975; Martonen 1993; Isaacs et al. 2005) during the different stages of the breathing cycle (inhalation, breath-hold, and expiration). Empirical equations are used to estimate the extrathoracic aerosol deposition (Rudolf et al. 1990; Grgic et al. 2004; Sandeau et al. 2010). As a result, this model yields generational particle deposition fractions, which, in turn, can be summed to give regional (TB and PU) and total values. Furthermore, deposition can be delineated by phase and mechanism (inertial impaction, sedimentation, and diffusion).

Input Data

Analytical modeling of deposition in lung airways is based on the straightforward premise that the physical and biological processes governing the behavior and fate of airborne drugs can be simulated if aerosol characteristics, ventilatory parameters, and lung morphologies are available. That is, these 3 families of parameters are fundamental to the description of aerosol transport and deposition processes; therefore, it is essential that

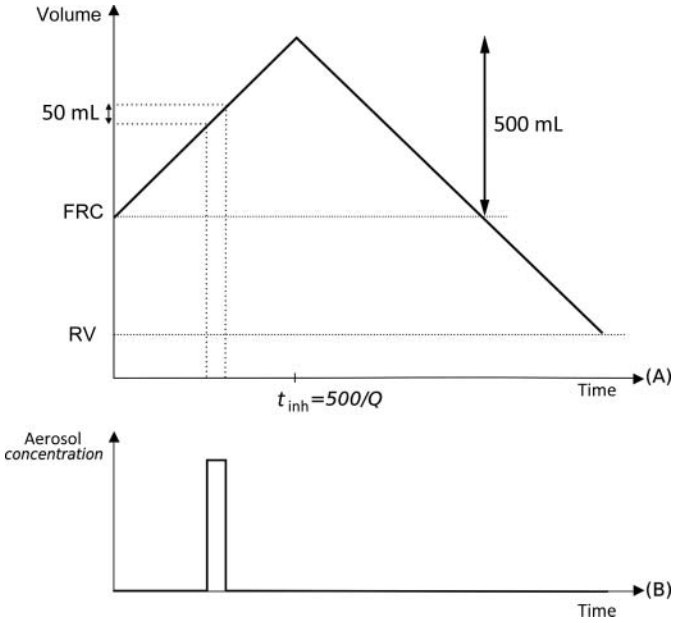

FIG. 1. Illustration of the serial bolus delivery method used in the KH experiments (Kim et al. 1996). At each maneuver, a TV of 500 mL is inhaled (see A); however, the aerosol is injected at prescribed points in small boluses of 50 mL (see B that is an idealized representation of the aerosol concentration at the exit of the device). The earlier the aerosol is injected during inhalation, the deeper it penetrates into the lungs. RV stands for residual volume.

the relevant experimental conditions are provided to perform a simulation.

Particle and Gas Characteristics

In the KH experiments, the generated aerosols of di-2-ethylexyl sebacate oil were particles of either 1, 3, or 5 μm in diameter, with geometrical standard deviation (GSD) of 1.15 and density of 0.91 g/cm^3 (Heyder et al. 1982). We assumed monodisperse, spherical, and nonhygroscopic particles.

The gas phase used in the KH experiments was air. The conditions of 1 atm and 37°C are assumed where the physical properties of interest are density (1.125 kg/m^3), absolute viscosity (18.95 μPa.s), and mean free path (67.8 nm).

Ventilation Parameters

An academic inhalation profile is assumed (Figure 1); thus, the ventilatory parameters needed to perform a simulation with our model are the tidal volume (TV), the inhalation time (combined to give the inhalation flow rate), the breath-hold (not used in the KH experiments, see Figure 3 of the original work, so set to zero), and the exhalation time.

Lung Morphology

The final category of input data concerns the descriptive model of the lung branching network. This aspect is treated in the following subsection.

Differentiation of Lung Morphology

Several models have been developed to describe the normal adult human lungs. One of the first models of the human respiratory tract geometry was derived by Weibel (1963). It is a symmetric and dichotomously branching network of cylindrical tubes, whose lengths, diameters, areas, and volumes are modeled by empirical equations. There are twenty-four generations of airways; each of them consisting in 2^n identical airways, where n is the generation number, 0 being the trachea. The morphology developed by Soong et al. (1979) (henceforth referred to as the Soong model) is based on Weibel's but is designed to account for inter- and intrasubject variability, and the airway dimensions are scaled to correspond to a more realistic FRC of 3200 mL. Indeed, the Weibel's model dimensions are based upon an FRC at 3/4 of the total lung capacity, whereas the typical value of FRC is about half of the total lung capacity.

In the Soong model, the FRC value of 3200 mL roughly corresponds to the mean value published in the guidelines of the International Commission on Radiological Protection (ICRP 1994) for an adult man from the general Caucasian population. However, FRC strongly depends on gender, age, and height of the subject (Stocks and Quanjer 1995) and mean values can be significantly different between populations (for the benefit of the reader, ICRP data are reproduced in Table 1). For instance, for an adult Caucasian woman, the mean FRC value given in ICRP is 2681 mL, which represents less than 84% of the value of the Soong model. In consequence, the Soong morphology should be adapted to fit the FRC. Moreover, it is reported in ICRP that the dimensions of the first 9 generations of the tracheobronchial tree (including the trachea) are related to body height. Consequently, we have developed a methodology adapting the Soong human lung model in order to take into account the variability of both FRC and body height between different populations or subjects.

Please note that we use the word population to designate any large category of subjects, such as the Caucasian adult male population. Subpopulation samples (e.g., the eleven male subjects enrolled in the KH experiments) are addressed as groups and may be composed of a few subjects to hundreds or thousands of subjects. Finally, any member of a group or a population is called an individual. The Soong lung model can be adapted

TABLE 1
Reference values for FRC and body height for different populations

	Adult male		Adult female	
	Height (m)	FRC (mL)	Height (m)	FRC (mL)
Caucasian	1.76	3300	1.63	2681
Japanese	1.70	2900	1.58	2050
Chinese	1.70	2950	1.58	2150

Note: Values are from ICRP (1994).

TABLE 2
Constant C values (used to calculate $SF_{0–8}$)

	Constant C	
Generation	Diameter	Length
0	0.540	0.559
1	0.530	0.468
2	0.507	0.474
3	0.489	0.502
4	0.429	0.431
5	0.441	0.476
6	0.452	0.441
7	0.405	0.359
8	0.333	0.273

Note: Values are from ICRP (1994).

for either a population (or a group), by using mean values of FRC and height obtained for the investigated population (or group), or for an individual, by taking into account his/her measured FRC and height. For the sake of simplicity, we will use the word population to present the methodology for adapting the Soong lung model to a given FRC and height, recognizing that the following steps are the same for a group or an individual.

The first step consists in scaling the diameter and length of the trachea and the first 8 bronchi (generations 0–8), as a function of the body height (ICRP 1994). The scaling factor by generation ($SF_{0–8}(g)$) is the ratio of airway diameter D (or length L) of a given generation g of the considered population compared to that in the reference Soong morphology. It is defined by:

$$SF_{0–8}(g) = \frac{D_{pop}(g)}{D_{Soong}(g)} = \frac{L_{pop}(g)}{L_{Soong}(g)} = C(g).(H - 1.76) + 1 \quad [1]$$

where $C(g)$ is a constant by generation (as given in Table 2) and H is the population's average height in meters.

From generations 9–23, a single factor is applied to the airway diameter and length, which is a function of the population's FRC mean value. This is based on the work of Hughes et al. (1972) who had shown a very close correlation between changes of the cube root of lung volume and both the bronchial length and diameter. Although this study was performed on excised dog lungs, it has been used as a starting point for lung scaling in humans (Segal et al. 2002; Martin and Finlay 2006). Consequently, to accommodate FRC variation, all airway diameters and lengths (hence the airway volumes) are modified by a uniform FRC scaling factor ($SF_{9–23}$) that is defined as the cube root of the ratio between the population's FRC (FRC_{pop}) and the Soong FRC (FRC_{Soong}):

$$SF_{9–23} = \frac{D_{pop}(g)}{D_{Soong}(g)} = \frac{L_{pop}(g)}{L_{Soong}(g)} = \left(\frac{FRC_{pop}}{FRC_{Soong}}\right)^{1/3} \quad [2]$$

The alveolar volume (V_{Apop}) of the scaled lung is deduced from the FRC value and the conducting volume V_{Cpop}:

$$V_{Apop} = FRC_{pop} - V_{Cpop} \quad [3]$$

where V_{Cpop} represents the conducting volume of the twenty-four generations, that is, the volume contained in the cylindrical part of the generation (as defined by the lengths and diameters).

The last step is the distribution of the alveolar volume per generation. The related scaling factor SF_A is defined for each alveolated generation g as the ratio between the alveolar volume of the considered generation and the total alveolar volume in the reference Soong morphology:

$$SF_A(g) = V_{ASoong}(g)/V_{ASoong} \quad [4]$$

where $V_{ASoong} = 2093.42$ mL. This factor is applied to all the alveolar volume from generations 17–23:

$$V_{Apop}(g) = SF_A(g).V_{Apop} \quad [5]$$

Following these steps, a lung morphology can be built for any healthy adult population, knowing the average height and FRC.

In the KH experiments, 2 groups were studied: eleven healthy adult males and eleven healthy adult females. Only the mean values for age and height for the 2 groups are reported in the Kim and Hu articles (Kim et al. 1988; Kim and Hu 1998) and are given in Table 3.

On the basis of these values, the theoretical FRC of each group was calculated by using the following equations (Stocks and Quanjer 1995):

$$\text{For the male group: } FRC = 2.34H + 0.01A - 1.09 \quad [6]$$

$$\text{For the female group: } FRC = 2.24H + 0.001A - 1.00 \quad [7]$$

where H is the height in meters and A is the age in years. These data are also reported in Table 3 for both groups. Given the mean height and the theoretical FRC of each group, 2 lung morphologies were built using the methodology described previously. Hence, we obtained one description of the respiratory tract representative of the male group (corresponding to a mean height

TABLE 3
Group characteristics and theoretical FRC values

Group	Age (years)	Height (m)	FRC (mL)
Male	25	1.81	3395.4
Female	25	1.67	2765.8

Note: Values are from Kim and Hu (1998) for age and body height. The theoretical FRC was calculated based on these values and the gender of the population.

TABLE 4
Description of the lung morphology for the male group

Airway generation	Number of airways	Airway diameter (cm)	Airway length (cm)	Generation conductive volume (cm^3)	Generation alveolar volume (cm^3)
0	1	1.617	10.788	22.36	0.00
1	2	1.095	4.260	8.15	0.00
2	4	0.744	1.701	3.03	0.00
3	8	0.502	0.681	1.11	0.00
4	16	0.402	1.135	2.40	0.00
5	32	0.313	0.958	2.48	0.00
6	64	0.250	0.804	2.73	0.00
7	128	0.205	0.677	3.17	0.00
8	256	0.165	0.567	3.50	0.00
9	512	0.137	0.482	4.30	0.00
10	1024	0.116	0.410	5.55	0.00
11	2048	0.097	0.348	7.04	0.00
12	4096	0.085	0.294	9.76	0.00
13	8192	0.073	0.241	12.07	0.00
14	16,384	0.066	0.205	15.64	0.00
15	32,768	0.059	0.178	19.89	0.00
16	65,536	0.054	0.147	25.17	0.00
17	13,1072	0.048	0.126	32.74	4.47
18	262,144	0.045	0.104	44.81	14.90
19	524,288	0.042	0.088	65.34	44.69
20	1,048,576	0.040	0.074	99.89	156.43
21	2,097,152	0.038	0.062	152.80	309.14
22	4,194,304	0.037	0.053	234.17	625.72
23	8,388,608	0.037	0.045	396.75	1065.22
			Total (mL):	1174.83	2220.57
			FRC (mL):	**3395.40**[*]	

[*]FRC in mL; the sum of the total conductive volume and the total alveolar volume.

of 1.81 m and an FRC of 3395.4 mL) and another one representative of the female group (corresponding to a mean height of 1.67 m and an FRC of 2765.8 mL). The airway dimensions and generation volumes for the male and female lung morphologies are described in Tables 4 and 5, respectively. Consequently, we can use these 2 representations of the human lung as input to our model to simulate the KH experiments.

Methodology of Simulation

The experimental dataset was obtained using a serial bolus aerosol delivery technique (Kim et al. 1996; Kim and Hu 1998) to measure regional deposition patterns of inhaled particles in the 2 healthy groups, for 3 flow rates and 3 particle diameters. For a given flow rate (Q) and a given particle size (D_p), each subject performed 10 inhalations of a 500-mL TV at a constant flow rate. An aerosol bolus was injected at different points during the inhalation in order to fill only 1/10 of the global TV (Figure 1). By this method, the aerosol is delivered to a specific volumetric depth (V_p) ranging from 50 to 500 mL. The aerosol number concentration was measured for each breath during inhalation and exhalation and used to calculate the bolus recovery (RC), that is, the fraction of exhaled particles compared with inhaled particles. For each subject and each configuration (Q and D_p), the fractional recovery was estimated for each bolus:

$$\mathrm{RC}_j = \frac{N_j}{N} \quad [8]$$

where N is the number of particles entering the lungs within a bolus and N_j is the number of particles exhaled after each particular inhalation.

The computer code used for this work was designed to compute aerosol deposition during continuous inhalation of air pollutant particle matter or nebulized therapeutic particles; therefore, the fractional bolus recovery RC_j is not a direct output. However, it can be related to the results of a series of continuous inhalation simulations. Subsequently, for each case (Q and D_p), 10 simulations have been realized with the following conditions: (1) the TV was equal to $i{\cdot}50$ mL (i being the index number of the simulation), (2) the inhalation time was set to $i{\cdot}50/Q$ s in

TABLE 5
Description of the lung morphology for the female group

Airway generation	Number of airways	Airway diameter (cm)	Airway length (cm)	Generation conductive volume (cm^3)	Generation alveolar volume (cm^3)
0	1	1.498	9.966	17.73	0.00
1	2	1.016	3.987	6.57	0.00
2	4	0.693	1.591	2.45	0.00
3	8	0.468	0.635	0.90	0.00
4	16	0.378	1.068	2.00	0.00
5	32	0.294	0.896	2.05	0.00
6	64	0.235	0.756	2.25	0.00
7	128	0.194	0.643	2.69	0.00
8	256	0.158	0.546	3.07	0.00
9	512	0.128	0.450	3.50	0.00
10	1024	0.108	0.383	4.52	0.00
11	2048	0.091	0.325	5.73	0.00
12	4096	0.079	0.275	7.95	0.00
13	8192	0.068	0.225	9.83	0.00
14	16,384	0.062	0.192	12.74	0.00
15	32,768	0.055	0.167	16.20	0.00
16	65,536	0.050	0.137	20.50	0.00
17	131,072	0.045	0.117	26.67	3.64
18	262,144	0.042	0.097	36.50	12.14
19	524,288	0.039	0.082	53.23	36.41
20	1,048,576	0.037	0.069	81.37	127.43
21	2,097,152	0.036	0.058	124.47	251.84
22	4,194,304	0.034	0.049	190.75	509.74
23	8,388,608	0.034	0.042	323.18	867.77
			Total (mL):	956.83	1808.97
			FRC (mL):	**2765.80***	

*FRC in mL; the sum of the total conductive volume and the total alveolar volume.

order to maintain a constant flow rate Q during the inhalation, and (3) the alveolar lung volume was increased to simulate the filling of the lungs due to the inhalation of fresh air prior to the aerosol. For each of these 10 simulations, the deposition fraction DF_i was calculated as a standard output from the code. This fraction, obtained from a continuous inhalation (since aerosol was injected throughout the inspiration maneuver), corresponds to the ratio of deposited particles to inhaled particles during the ith simulation. The relation between the DF_is, computed by our code, and RC_j, as measured by Kim et al. (1996, 1998) and given in Equation (8), is for $j = i$:

$$RC_j = i(1 - DF_i) - (i - 1)(1 - DF_{i-1}) \quad [9]$$

On the basis of the measured RC_js, the TDF can be calculated for the equivalent inhalation with continuous nebulization using the following equation:

$$TDF = 1 - \frac{1}{n}\sum_{j=1}^{n} RC_j \quad [10]$$

where n is the number of inhalation experiments ($n = 10$ in the KH experiments).

As the aerosol is continuously inhaled in our simulations, the TDF is a direct output from the code from the 10th simulation (DF_{10}), whereas the experimental value of the TDF is deduced from the 10 RC measurements, using Equation (10) where $n = 10$.

Thus, analytical simulations can be used to calculate the bolus recovery and TDF in order to be compared with the results from the KH experiments based on the aerosol bolus delivery technique. In addition, predicted results can be computed for the 2 different groups using the 2 morphologies presented previously.

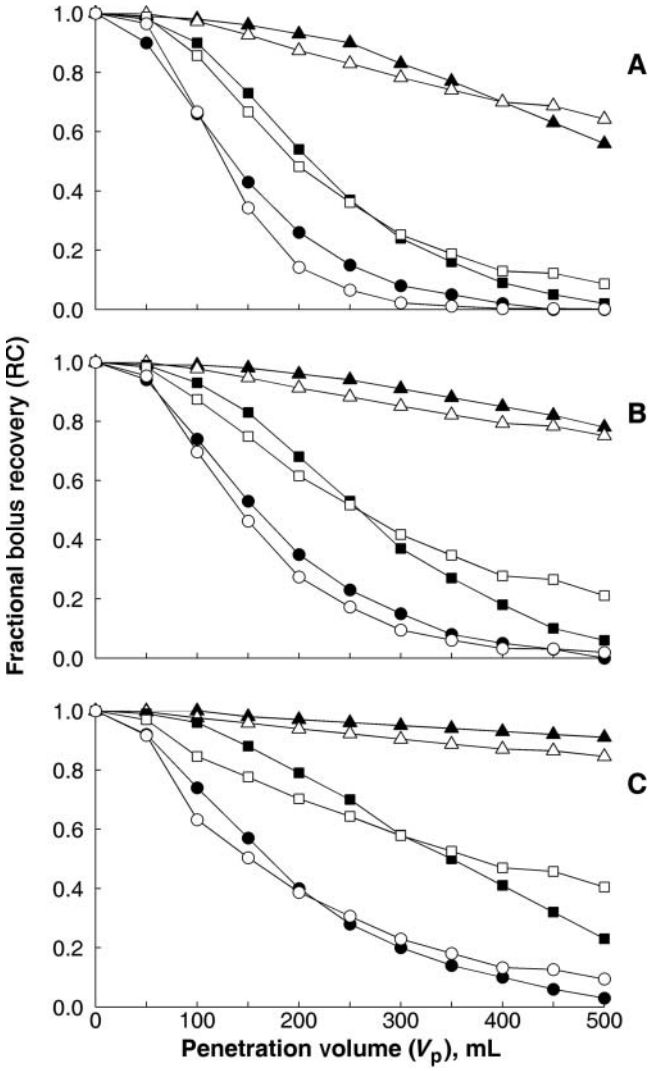

FIG. 2. Fractional bolus recovery (RC) in the male group as a function of penetration volume (V_p). Experimental values (black solid symbols) and predicted data (open symbols) are presented for particles of 1 μm (triangle), 3 μm (square), and 5 μm (circle) in diameter with 3 flow rates: 150 mL/s (A), 250 mL/s (B), and 500 mL/s (C).

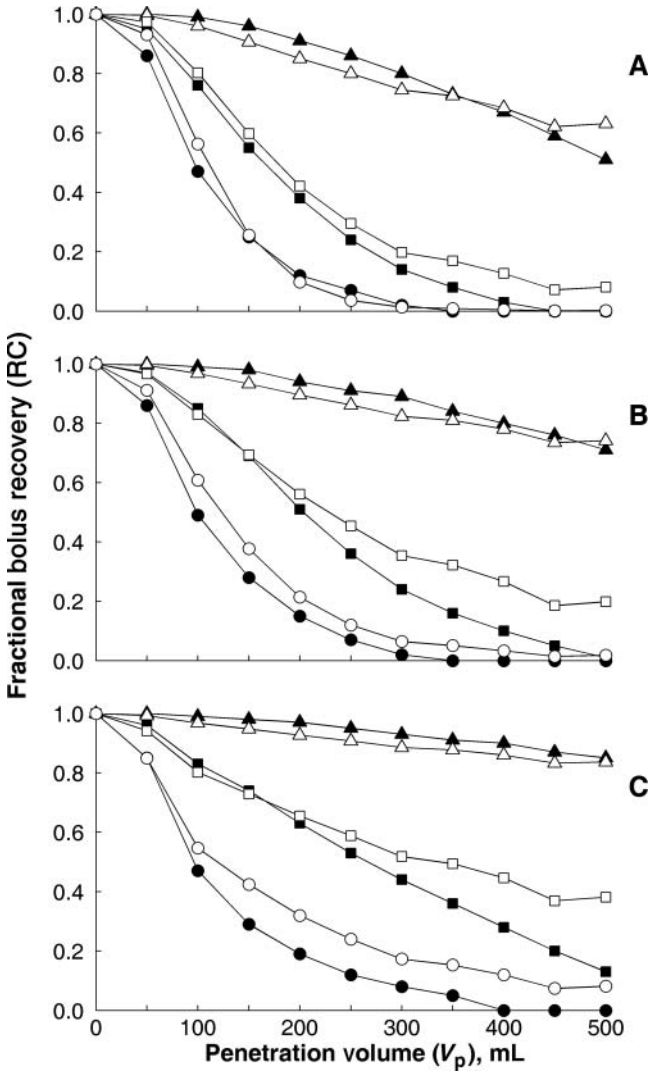

FIG. 3. Fractional bolus recovery (RC) in the female group as a function of penetration volume (V_p). Experimental values (black solid symbols) and predicted data (open symbols) are presented for particles of 1 μm (triangle), 3 μm (square), and 5 μm (circle) in diameter with 3 flow rates: 150 mL/s (A), 250 mL/s (B), and 500 mL/s (C).

RESULTS

The predicted and experimental fractional bolus recovery is plotted as a function of penetration volume (V_p) for particles of 1, 3, and 5 μm diameter, and for 3 flow rates ($Q = 150, 250$, and 500 mL/s), for the male and female groups, in Figures 2 and 3, respectively. Note that for a given set of experimental conditions (group, Q, and D_p), the experimental values are an average of the data obtained for the eleven subjects of the concerned group, whereas the predicted values have been obtained with a single morphological model representative of the eleven subjects. Furthermore, the 10 measurements have been acquired during 10 successive and independent inspiratory/expiratory maneuvers (repeated 5 times), while the predicted results have been established through the compilation of the results of a series of 10 simulations.

Nevertheless, computed and experimental results are in very good agreement. As commented by Kim and Hu in their article (1998), "RC decreased monotonically with increasing V_p for each particle size and [flow rate] used, but the decrease of RC was greater with particles of larger size in both men and women. [. . .] RC values were smaller with lower [flow rate] (i.e., longer residence time) for a given value of D_p." This behavior is predicted by the model, except for the largest penetration volume for the female group.

Both experimental and simulated TDF data are presented for male and female groups in Figures 4 and 5, respectively, for the 3 investigated flow rates and particle sizes. Globally, the

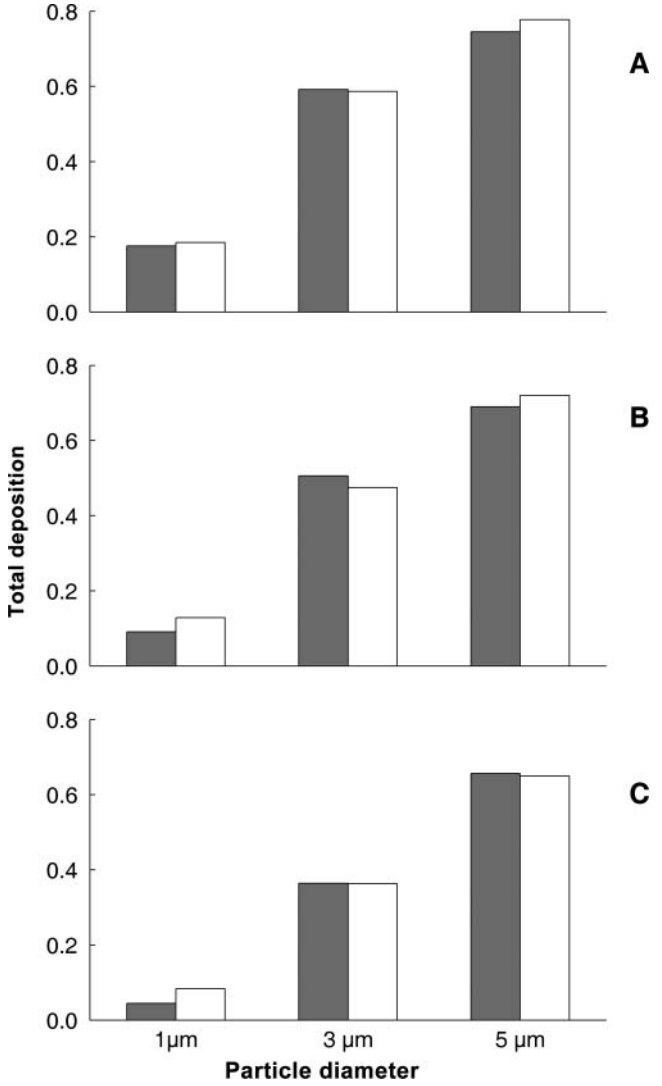

FIG. 4. TDF in the male group. Experimental values (gray bars) and predicted data (white bars) are presented for 3 particle sizes (1, 3, and 5 μm) and 3 different flow rates: 150 mL/s (A), 250 mL/s (B), and 500 mL/s (C).

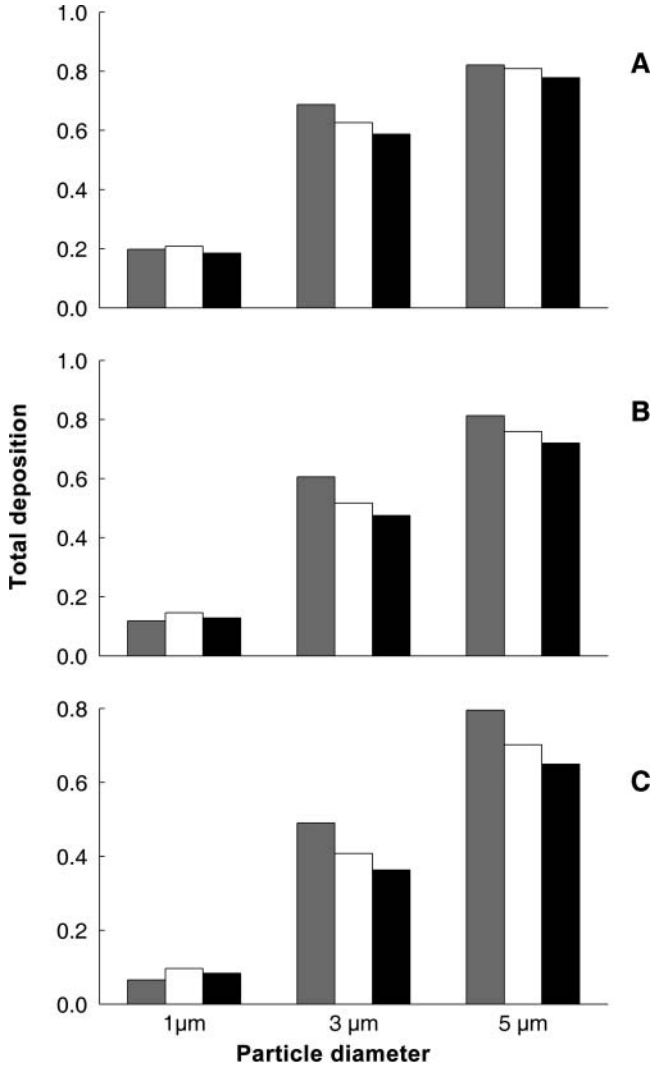

FIG. 5. TDF in the female group. Experimental values (gray bars) are compared with predicted data obtained with a female lung morphology (white bars) and predicted data obtained with a male lung morphology (black bars). Data are presented for 3 particle sizes (1, 3, and 5 μm) and 3 different flow rates: 150 mL/s (A), 250 mL/s (B), and 500 mL/s (C).

main tendencies described by Kim and Hu (1998) about their experimental results can also be observed in the predicted data; namely, our model similarly predicted (1) a decrease in aerosol deposition with increasing flow rate for the same particle size, (2) an increase in particle deposition with increasing particle size for the same flow rate, and (3) a greater increase in aerosol deposition by increasing particle size than by decreasing the flow rate. These qualitative observations are true for both groups.

Concerning gender effects for the male group, predicted TDF values correlate very well with measurements, especially for coarse particles: the absolute difference ranges between 0.3% and 6.6% for 3 μm particles and between 1.1% and 4.2% for 5 μm particles. However, the computed TDF for 1 μm particles is greater than experimental values by 5.0%, 29.4%, and 46.8% for $Q = 150$, 250, and 500 mL/s, respectively. The computed values for the female group show slightly less agreement with experimental data than for the male group. The absolute difference ranges between 9.7%–20.2% and 1.5%–13.3% for coarse particles of 3 and 5 μm, respectively. For the smallest particles, the computed TDF is greater than experimental values by 4.9%, 18.7%, and 32.7% for flow rates of 150, 250, and 500 mL/s, respectively. When comparing total aerosol deposition in male and female groups, we can observe that both experimentally and theoretically, TDF is greater in women than in men, for all diameters and all flow rates. However, the predicted increase is smaller than the measured value. Indeed, the increase in aerosol deposition in women compared with men is between 5.3% and 28.7% experimentally (depending on the flow rate and particle size) and between 3.8% and 13.5% theoretically (for the same flow rates and particle sizes).

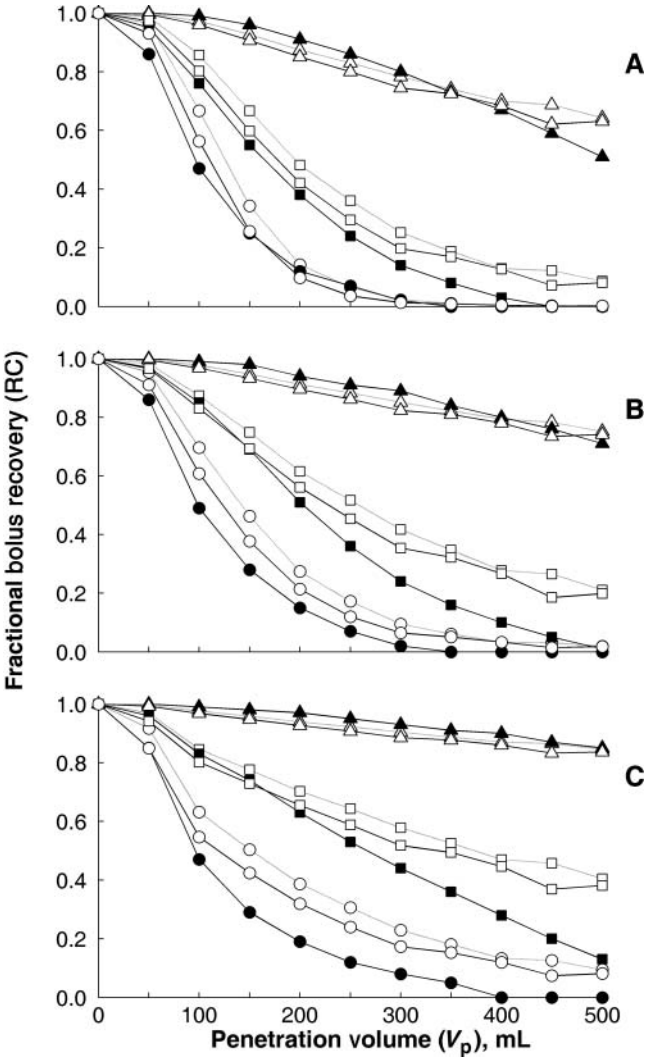

FIG. 6. Fractional bolus recovery (RC) as a function of penetration volume (V_p) for particles of 1 μm (triangle), 3 μm (square), and 5 μm (circle) in diameter, for various flow rates: 150 mL/s (A), 250 mL/s (B), and 500 mL/s (C). Experimental values for the female group (black solid symbols) are compared with predicted data obtained with a female lung morphology (solid connecting line with open symbols) and predicted data obtained with a male lung morphology (dashed connecting line with open symbols).

In Figure 6, a direct comparison between male and female groups is shown for fractional bolus recovery as a function of penetration volume, for all flow rates and all particle sizes. The experimental values for the female group are plotted on the same figure as the predicted RC values obtained with our model when using either the male or the female lung morphology. The predicted results are more consistent with experimental data when the respiratory tract morphology was adapted to the investigated group.

As shown in Figure 5, when the female lung morphology is used, the predicted TDF correlates better with the measured value (except for 1 μm particles for flow rates of 250 and 500 mL/s). For instance, the TDF value for 5 μm particles with a flow rate of 150 mL/s is overestimated by 1.4% when using our code with the female morphology. It would be overpredicted by 5.2% if the morphology had not been adapted to the female population's characteristics.

DISCUSSION

The motivation for the work described herein arose from the fact that the Soong morphometric model was adapted from the Weibel (1963) model that was based almost exclusively on casts from adult males aged fifty years or older. As inhalation exposures are not systematically performed on male subjects of this age, we are convinced that it is useful to provide a methodology to adapt this standard model to other types of populations, such as the subjects enrolled in the KH experiments who were younger (25 years old on average) and who were female for one of the 2 groups.

To our knowledge, this study is the first attempt of comparison between predicted values from an analytical model and measured values of regional aerosol deposition in male and female groups. Overall, a good agreement can be observed between predicted and experimental results, for RC and TDF, for different flow rates and particle diameters. However, some discrepancies still remain.

The largest differences between experimental and simulated TDF results are obtained for 1 μm particles. This divergence could be due to the modeling of the true expiratory maneuver. Indeed, in the KH experiments, the respiratory maneuver consisted of a continuous exhalation to the residual volume at a constant flow rate. But in our simulations, the expiratory maneuver was set equal to the inspiratory volume of 500 mL with a constant flow rate, hence reaching the FRC that is greater than the residual volume (corresponding to the lung volume at the end of a forced expiratory exhalation). As discussed in Kim et al. (1996), this maximal expiration to residual volume may result in lower deposition than expected with steady-state breathing, especially for 1 μm particles with small deposition efficiency. Moreover, the deposition values for this particle size are minimal, especially for the highest flow rate, and are perhaps within the experimental uncertainties associated with human subject experiments (Stahlhofen et al. 1981; Peterson et al. 2008). For coarse particles, a good correlation can be observed between experimental and predicted TDF values; nevertheless, important discrepancies exist for RC data, especially for 3 μm particles. Once again, this may be due to the simulated expiratory maneuver: as a longer expiration time associated with a constant flow rate can induce changes in the deposition pattern, a series of simulations based on a complete expiratory pattern could produce greater levels of regional deposition, especially for 3 μm particles that are the more likely to be deposited by sedimentation during the exhalation process. This is illustrated in Figure 7 where the deposition fraction is plotted for both inhalation and exhalation phases on a generational basis (i.e., from 0 to 23 during inspiration and from 23 to 0 during expiration).

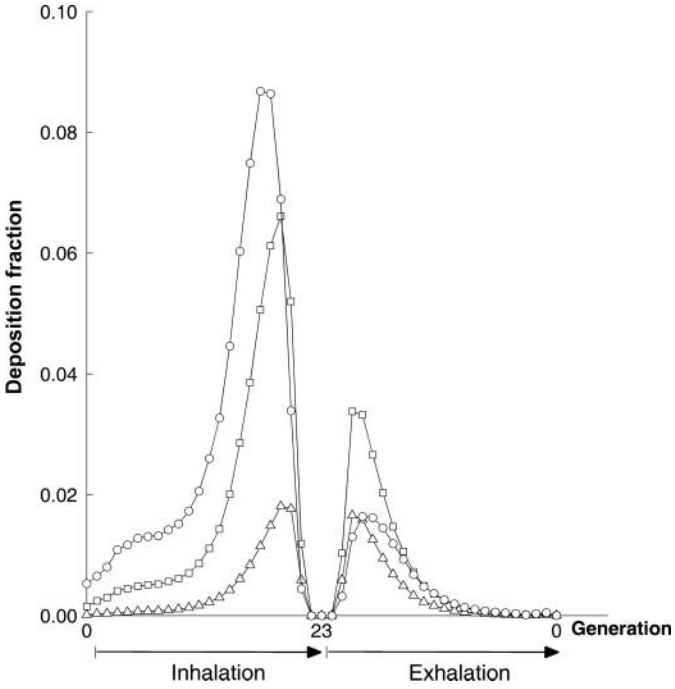

FIG. 7. Predicted deposition of particles of 1 μm (triangle), 3 μm (square), and 5 μm (circle) in diameter, for a flow rate of 150 mL/s. The data are obtained with the male lung morphology and are presented on a generational basis for both inhalation and exhalation phases.

The results are given for the 3 particle sizes, for a flow rate of 150 mL/s, and using the male lung morphology. We can observe that the deposition fraction of 3 μm particles during the exhalation phase is greater than that of 1 and 5 μm particles, making it more sensitive to inconsistencies between the simulated and experimental conditions during exhalation.

Another difference between the experiments and the simulations is related to the not-continuous injection of aerosol specific to the bolus technique. As previously mentioned, the code we used had not been designed to allow this kind of inhalation process, so the results of 2 independent simulations were needed to obtain the equivalent bolus recovery factor of one *in vivo* inhalation experiment. However, we believe that using a code capable of simulating not-continuous inhalation of aerosol would have made things easier (1 simulation for 1 experiment) but would not have modified the results. Existing models computing bolus aerosol delivery (Darquenne and Paiva 1994; Darquenne et al. 1997) are generally used to investigate the bolus dispersion (i.e., a discrete bolus is inhaled but is dissipated during exhalation) and lung anatomy. As this phenomenon of nonconvective transport of the aerosol is not accounted for in our model, it may be one of the factors contributing to differences between our results and the experimental data.

The large intersubject variability in terms of aerosol deposition pattern has been widely reported in the peer-reviewed literature. Among the criteria identified as influential parameters is the breathing pattern, when the ventilatory regime is spontaneous and not controlled (Kim and Jaques 2004; Kim and Hu 2006). Another source of variability in aerosol deposition pattern is related to the differences in lung morphologies. These differences can be due to malformations of the lungs owing to smoking or disease (Kim et al. 1988; Bennett et al. 1997; Kim and Kang 1997; Brown et al. 2002), but they also appear in healthy populations when considering various ages and gender (Pritchard et al. 1986; Kim et al. 1988; Bennett et al. 1996; Kim and Hu 1998; Jaques and Kim 2000; Kim and Jaques 2004; Kim and Jaques 2005). A parameter that is related to the age and gender and that enables rough categorization of lung morphology in terms of volume is the FRC. Reference values can be found in ICRP for Caucasian, Japanese, and Chinese populations for both males and females. The difference in reference FRC between male Caucasians and female Chinese, for instance, is 53% (see Table 1) and justifies our concern about categorization of lung morphology for different populations. Moreover, the FRC has been shown to have a large influence on aerosol deposition patterns (Segal et al. 2000; Hofmann et al. 2002), substantiating the importance of the morphology categorization process we have developed, which allows morphometric data (height) and respiratory tract characteristics (FRC) to be incorporated directly in the lung model, instead of being used to modify the results afterward (Martin and Finlay 2006).

Nevertheless, as FRC values were not available for each subject studied in the KH experiments, we were required to estimate the mean FRC of each group using averaged values of age and height to build the average lung morphology. If the characteristics (i.e., FRC and height) of the eleven subjects enrolled in each of the 2 groups had been available, we could have built eleven morphologies and performed eleven series of simulations for each group. Hence, it would have been interesting to compare the mean experimental data with the average of our computed results for each group, and thus to investigate the intersubject variability. Moreover, we determined the FRC of each group using equations based on age, height, and gender that have a limited validity. They apply for a height range of 1.55–1.95 m in men, and 1.45–1.80 m in women, and are applicable between ages 18 and 70 years. As the average height of each group was only available, we could be out of range for 1 or several subject(s). Furthermore, these equations do not apply for pregnant women who have a reduced FRC compared with nonpregnant women (Garcia-Rio et al. 1996; Nelson–Piercy 2001), and as the size of the lungs varies with ethnic group (Yang et al. 1991; Cotes 1993), they are only available for Caucasians. Consequently, individual FRC values are useful information and we recommend that they should be made available when reporting results from human subject experiments.

Globally, the results obtained when simulating aerosol delivery in the male group are in better agreement with the experimental values than that in the female group. This may denote that the female lung morphology needs more complicated scaling than simply a height adaptation, or more precisely, a specific modification of the length and diameter of their airways, as they

may be smaller in females than in males of the same stature, particularly in the upper airways and the trachea (Martin et al. 1987). However, our approach toward modeling was to start with an existing methodology from the literature.

At this point, we would like to emphasize that the FRC may not be sufficient to characterize and represent the anatomical differences in human lungs. Some specifics regarding this complex structure are not described in the Soong model, for instance, its asymmetric structure, the occurrence of trifurcations (Cohen et al. 1990), the tracheal shape (Mehta and Myat 1984), and the differences in the main bifurcation angle (Karabulut 2005). In order to build a specific lung model for an individual, it may be necessary to use detailed characteristics of the subject's lung morphology—coming from medical images—to better represent his/her lung morphology (Vial et al. 2005). The prediction of aerosolized drug transport and deposition would be realized in this patient-specific morphology and would help to adapt and optimize the treatment and lead to customized aerosol therapy regimens.

In this article, we deliberately compared predicted results for male and female deposition patterns only for assessing the relevance of the adaptation of the Soong model with various populations. It is beyond the scope of this article to draw more general conclusions of the gender effect on drug deposition patterns. For example, the controlled breathing patterns used in our simulations, based on the reported experimental parameters, imply the same inhaled TV for both populations; however, it represents a relatively deeper inhalation for females (with smaller FRC than males). It is also recognized that spontaneous breathing patterns for males and females are different, as well as those for other populations.

In conclusion, we presented a methodology to modify the classic Soong model in order to take into account physiological parameters such as FRC and height. This methodology can be used to create lung morphologies adapted to populations (or groups) exhibiting a mean FRC value different than 3200 mL and/or a mean height value different than 1.76 m. This categorization of lung morphologies has been used along with an analytical model to compute aerosol deposition for 2 groups (male and female) enrolled in the KH experiments. The results have been found to correlate better with the associated experimental measurements, for various flow rates and particle sizes, with the use of the adapted morphologies. This advance in the simulation of respiratory drug delivery should help to adapt aerosol therapy protocols to the population considered; in other words, gender-specific, age-specific, and ethnic-specific treatments may have a sound scientific foundation.

REFERENCES

Anjilvel, S., and Asgharian, B. (1995). A Multiple-Path Model of Particle Deposition in the Rat Lung. *Fundam. Appl. Toxicol.*, 28:41–50.

Asgharian, B., Hofmann, W., and Bergmann, R. (2001). Particle Deposition in a Multiple-Path Model of the Human Lung. *Aerosol Sci. Tech.*, 34:332–339.

Bennett, W. D., Scheuch, G., Zeman, K. L., Brown, J. S., Kim, C., Heyder, J., et al. (1998). Bronchial Airway Deposition and Retention of Particles in Inhaled Boluses: Effect of Anatomic Dead Space. *J. Appl. Physiol.*, 85:685–694.

Bennett, W. D., Scheuch, G., Zeman, K. L., Brown, J. S., Kim, C., Heyder, J., et al. (1999). Regional Deposition and Retention of Particles in Shallow, Inhaled Boluses: Effect of Lung Volume. *J. Appl. Physiol.,* 86:168–173.

Bennett, W. D., Zeman, K. L., and Kim, C. (1996). Variability of Fine Particle Deposition in Healthy Adults: Effect of Age and Gender. *Am. J. Respir. Crit. Care Med.,* 153:1641–1647.

Bennett, W. D., Zeman, K. L., Kim, C. S., and Mascarella, J. (1997). Enhanced Deposition of Fine Particles in COPD Patients Spontaneously Breathing at Rest. *Inhal. Toxicol.,* 9:1–14.

Brown, J. S., Zeman, K. L., and Bennett, W. D. (2002). Ultrafine Particle Deposition and Clearance in the Healthy and Obstructed Lung. *Am. J. Respir. Crit. Care Med.,* 166:1240–1247.

Choi, J., and Kim, C. S. (2007). Mathematical Analysis of Particle Deposition in Human Lungs: An Improved Single Path Transport Model. *Inhal. Toxicol.,* 19:925–939.

Cohen, B. S., Sussman, R. G., and Lippmann, M. (1990). Ultrafine Particle Deposition in a Human Tracheobronchial Cast. *Aerosol Sci. Tech.,* 12:1082–1091.

Cotes, J. E. (1993). *Lung Function: Assessment and Application in Medicine*. Blackwell Scientific Publication, Oxford.

Darquenne, C., Brand, P., Heyder, J., and Paiva, M. (1997). Aerosol Dispersion in Human Lung: Comparison between Numerical Simulations and Experiments for Bolus Tests. *J. Appl. Physiol.,* 83:966–974.

Darquenne, C., and Paiva, M. (1994). One-Dimensional Simulation of Aerosol Transport and Deposition in the Human Lung. *J. Appl. Physiol.,* 77:2889–2898.

Farkas, A., and Balashazy, I. (2008). Quantification of Particle Deposition in Asymmetrical Tracheobronchial Model Geometry. *Comput. Biol. Med.,* 38:508–518.

Finlay, W. H., and Martin, A. R. (2008). Recent Advances in Predictive Understanding of Respiratory Tract Deposition. *J. Aerosol Med. Pulm. Drug Deliv.,* 21:189–205.

Garcia-Rio, F., Pino, J. M., Gomez, L., varez-Sala, R., Villasante, C., and Villamor, J. (1996). Regulation of Breathing and Perception of Dyspnea in Healthy Pregnant Women. *Chest,* 110:446–453.

Grgic, B., Finlay, W. H., Burnell, P. K. P., and Heenan, A. F. (2004). In Vitro Intersubject and Intrasubject Deposition Measurements in Realistic Mouth-Throat Geometries. *J. Aerosol Sci.,* 35:1025–1040.

Heyder, J. (2004). Deposition of Inhaled Particles in the Human Respiratory Tract and Consequences for Regional Targeting in Respiratory Drug Delivery. *Proc. Am. Thorac. Soc.,* 1:315–320.

Heyder, J., Armbruster, L., Gebhart, J., Grein, E., and Stahlhofen, W. (1975). Total Deposition of Aerosol Particles in the Human Respiratory Tract for Nose and Mouth Breathing. *J. Aerosol Sci.,* 6:311–328.

Heyder, J., Gebhart, J., Rudolf, G., Schiller, C. F., and Stahlhofen, W. (1986). Deposition of Particles in the Human Respiratory Tract in the Size-Range 0.005-15μm. *J. Aerosol Sci.,* 17:811–825.

Heyder, J., Gebhart, J., Stahlhofen, W., and Stuck, B. (1982). Biological Variability of Particle Deposition in the Human Respiratory Tract During Controlled and Spontaneous Mouth-Breathing. *Ann. Occup. Hyg.,* 26:137–147.

Hofmann, W., Asgharian, B., and Winkler–Heil, R. (2002). Modeling Intersubject Variability of Particle Deposition in Human Lungs. *J. Aerosol Sci.,* 33:219–235.

Howarth, P. H. (2001). Why Particle Size Should Affect Clinical Response to Inhaled Therapy. *J. Aerosol Med.,* 14:S27–S34.

Hughes, J. M., Hoppin, F. G., Jr., and Mead, J. (1972). Effect of Lung Inflation on Bronchial Length and Diameter in Excised Lungs. *J. Appl. Physiol.,* 32:25–35.

ICRP (1994). Human Respiratory Tract Model for Radiological Protection. *Ann. ICRP,* 24:1–3.

Ingham, D. B. (1975). Diffusion of Aerosols from a Stream Flowing through a Cylindrical Tube. *Aerosol Sci.*, 6:125–132.

Isaacs, K. K., Rosati, J. A., and Martonen, T. B. (2005). Mechanisms of Particle Deposition, in *Aerosols Handbook: Measurement, Dosimetry, and Health*

Effects, L. S. Ruzer and N. H. Harley, eds., CRC Press, Boca Raton, FL, pp. 75–99.

Jaques, P. A., and Kim, C. S. (2000). Measurement of Total Lung Deposition of Inhaled Ultrafine Particles in Healthy Men and Women. *Inhal. Toxicol.,* 12:715–731.

Karabulut, N. (2005). CT Assessment of Tracheal Carinal Angle and Its Determinants. *Br. J. Radiol.,* 78:787–790.

Katz, I. M., and Martonen, T. B. (1996). Three-Dimensional Fluid Particle Trajectories in the Human Larynx and Trachea. *J. Aerosol Med.,* 9:513–520.

Katz, I. M., Schroeter, J. D., and Martonen, T. B. (2001). Factors Affecting the Deposition of Aerosolized Insulin. *Diabetes Tech. Therapeut.,* 3:387–397.

Kim, C. S. (2000). Methods of Calculating Lung Delivery and Deposition of Aerosol Particles. *Respir. Care,* 45:695–711.

Kim, C. S., and Hu, S. C. (1998). Regional Deposition of Inhaled Particles in Human Lungs: Comparison between Men and Women. *J. Appl. Physiol.,* 84:1834–1844.

Kim, C. S., and Hu, S. C. (2006). Total Respiratory Tract Deposition of Fine Micrometer-Sized Particles in Healthy Adults: Empirical Equations for Sex and Breathing Pattern. *J. Appl. Physiol.,* 101:401–412.

Kim, C. S., Hu, S. C., DeWitt, P., and Gerrity, T. R. (1996). Assessment of Regional Deposition of Inhaled Particles in Human Lungs by Serial Bolus Delivery Method. *J. Appl. Physiol.,* 81:2203–2213.

Kim, C. S., and Jaques, P. A. (2004). Analysis of Total Respiratory Deposition of Inhaled Ultrafine Particles in Adult Subjects at Various Breathing Patterns. *Aerosol Sci. Tech.,* 38:525–540.

Kim, C. S., and Jaques, P. A. (2005). Total Lung Deposition of Ultrafine Particles in Elderly Subjects during Controlled Breathing. *Inhal. Toxicol.,* 17:387–399.

Kim, C. S., and Kang, T. C. (1997). Comparative Measurement of Lung Deposition of Inhaled Fine Particles in Normal Subjects and Patients with Obstructive Airway Disease. *Am. J. Respir. Crit. Care Med.,* 155:899–905.

Kim, C. S., Lewars, G. A., and Sackner, M. A. (1988). Measurement of Total Lung Aerosol Deposition As an Index of Lung Abnormality. *J. Appl. Physiol.,* 64:1527–1536.

Labiris, N. R., and Dolovich, M. B. (2003). Pulmonary Drug Delivery. Part I: Physiological Factors Affecting Therapeutic Effectiveness of Aerosolized Medications. *Br. J. Clin. Pharmacol.,* 56:588–599.

Longest, P. W., and Vinchurkar, S. (2007). Validating CFD Predictions of Respiratory Aerosol Deposition: Effects of Upstream Transition and Turbulence. *J. Biomech.,* 40:305–316.

Martin, T. R., Castile, R. G., Fredberg, J. J., Wohl, M. E., and Mead, J. (1987). Airway Size Is Related to Sex but Not Lung Size in Normal Adults. *J. Appl. Physiol.,* 63:2042–2047.

Martin, A. R., and Finlay, W. H. (2006). A General, Algebraic Equation for Predicting Total Respiratory Tract Deposition of Micrometer-Sized Aerosol Particles in Humans. *J. Aerosol Sci.,* 38:246–253.

Martonen, T. B. (1982). Analytical Model of Hygroscopic Particle Behavior in Human Airways. *Bull. Math. Biol.,* 44:425–442.

Martonen, T. B. (1993). Mathematical Model for the Selective Deposition of Inhaled Pharmaceuticals. *J. Pharmaceut. Sci.,* 82:1191–1199.

Martonen, T. B., and Katz, I. M. (1993). Deposition Patterns of Aerosolized Drugs within Human Lungs: Effects of Ventilatory Parameters. *Pharmaceut. Res.,* 10:871–878.

Martonen, T., Katz, I., and Cress, W. (1995). Aerosol Deposition As a Function of Airway Disease: Cystic Fibrosis. *Pharmaceut. Res.,* 12:96–102.

Martonen, T. B., Musante, C. J., Segal, R. A., Schroeter, J. D., Hwang, D., Dolovich, M. A., et al. (2000). Lung Models: Strengths and Limitations. *Respir. Care,* 45:712–736.

Martonen, T. B., Rosati, J. A., and Isaacs, K. K. (2005a). Modeling Deposition of Inhaled Particles, in *Aerosols Handbook: Measurement, Dosimetry, and Health Effects*, L. S. Ruzer and N. H. Harley, eds., CRC Press, Boca Raton, FL, pp. 113–155.

Martonen, T. B., Smyth, H. D., Isaacs, K. K., and Burton, R. T. (2005b). Issues in Drug Delivery: Concepts and Practice. *Respir. Care,* 50:1228–1252.

Mehta, S., and Myat, H. M. (1984). The Cross-Sectional Shape and Circumference of the Human Trachea. *Ann. Roy. Coll. Surg.,* 66:356–358.

Muir, D. C. F., and Cena, K. (1987). Deposition of Ultrafine Aerosols in the Human Respiratory Tract. *Aerosol Sci. Tech.,* 6:183–190.

Nelson–Piercy, C. (2001). Asthma in Pregnancy. *Thorax,* 56:325–328.

Oldham, M. J. (2010). Dosimetry Implications of Uncertainties in Lung Architecture: Is Weibel Good Enough? *RDD 2010 Proc.,* 1:205–214.

Peterson, J. B., Prisk, G. K., and Darquenne, C. (2008). Aerosol Deposition in the Human Lung Periphery Is Increased by Reduced-Density Gas Breathing. *J. Aerosol Med. Pulm. Drug Deliv.,* 21:159–168.

Phalen, R. F., Schum, M., and Oldham, M. J. (1990). The Sensitivity of an Inhaled Aerosol Tracheobronchial Deposition Model to Input Parameters. *J. Aerosol Med.,* 3:271–282.

Pritchard, J. N. (2001). The Influence of Lung Deposition on Clinical Response. *J. Aerosol Med.,* 14:S19–S26.

Pritchard, J. N., Jefferies, S. J., and Black, A. (1986). Sex Differences in the Regional Deposition of Inhaled Particles in the 2.5–7.5 μm Size Range. *J. Aerosol Sci.,* 17:385–389.

Rudolf, G., Köbrich, R., and Stahlhofen, W. (1990). Modelling and Algebraic Formulation of Regional Aerosol Deposition in Man. *J. Aerosol Sci.,* 21:S403–S406.

Sandeau, J., Katz, I., Fodil, R., Louis, B., Apiou-Sbirlea, G., Caillibotte, G., et al. (2010). CFD Simulation of Particle Deposition in a Reconstructed Human Oral Extrathoracic Airway for Air and Helium-Oxygen Mixtures. *J. Aerosol Sci.,* 41:281–294.

Sbirlea-Apiou, G., Lemaire, M., Katz, I., Conway, J., Fleming, J., and Martonen, T. (2004). Simulation of the Regional Manifestation of Asthma. *J. Pharmaceut. Sci.,* 93:1205–1216.

Schiller, C. F., Gebhart, J., Heyder, J., Rudolf, G., and Stahlhofen, W. (1988). Deposition of Monodisperse Insoluble Aerosol Particles in the 0.005 to 0.2 μm Size Range within the Human Respiratory Tract. *Ann. Occup. Hyg.,* 32:41–49.

Segal, R. A., Martonen, T. B., and Kim, C. S. (2000). Comparison of Computer Simulations of Total Lung Deposition to Human Subject Data in Healthy Test Subjects. *J. Air Waste Manag. Assoc.,* 50:1262–1268.

Segal, R. A., Martonen, T. B., Kim, C. S., and Shearer, M. (2002). Computer Simulations of Particle Deposition in the Lungs of Chronic Obstructive Pulmonary Disease Patients. *Inhal. Toxicol.,* 14:705–720.

Soong, T. T., Nicolaides, P., Yu, C. P., and Soong, S. C. (1979). A Statistical Description of the Human Tracheobronchial Tree Geometry. *Respir. Physiol.,* 37:161–172.

Stahlhofen, W., Gebhart, J., and Heyder, J. (1980). Experimental Determination of the Regional Deposition of Aerosol Particles in the Human Respiratory Tract. *Am. Ind. Hyg. Assoc. J.,* 41:385–398.

Stahlhofen, W., Gebhart, J., and Heyder, J. (1981). Biological Variability of Regional Deposition of Aerosol Particles in the Human Respiratory Tract. *Am. Ind. Hyg. Assoc. J.,* 42:348–352.

Stocks, J., and Quanjer, P. H. (1995). Reference Values for Residual Volume, Functional Residual Capacity and Total Lung Capacity. ATS Workshop on Lung Volume Measurements. Official Statement of The European Respiratory Society. *Eur. Respir. J.,* 8:492–506.

Stuart, B. O. (1984). Deposition and Clearance of Inhaled Particles. *Environ. Health Perspect.,* 55:369–390.

Taulbee, D. B., and Yu, C. P. (1975). A Theory of Aerosol Deposition in the Human Respiratory Tract. *J. Appl. Physiol.,* 38:77–85.

Vial, L., Perchet, D., Fodil, R., Caillibotte, G., Fetita, C., Preteux, F., et al. (2005). Airflow Modeling of Steady Inspiration in Two Realistic Proximal Airway Trees Reconstructed from Human Thoracic Tomodensitometric Images. *Comput. Meth. Biomech. Biomed. Eng.,* 8:267–277.

Weibel, E. R. (1963). *Morphometry of the Human Lung*. Springer-Verlag, Berlin.

Xi, J., Longest, P. W., and Martonen, T. B. (2008). Effects of the Laryngeal Jet on Nano- and Microparticle Transport and Deposition in an Approximate Model of the Upper Tracheobronchial Airways. *J. Appl. Physiol.,* 104:1761–1777.

Yang, T. S., Peat, J., Keena, V., Donnelly, P., Unger, W., and Woolcock, A. (1991). A Review of the Racial Differences in the Lung Function of Normal Caucasian, Chinese and Indian Subjects. *Eur. Respir. J.,* 4:872–880.